

# A combined distance and surface profile measurement system for industrial applications: a European project

F Docchio†, U Perini‡ and H Tiziani§

† Dipartimento di Elettronica per l'Automazione, Università degli Studi di Brescia, Via Branze 38, I-25123 Brescia, Italy

‡ Sezione Diagnostica Elettroottica, CISE SpA, Via Reggio Emilia 39, I-20134 Milano, Italy

§ Institut für technische Optik, Universität Stuttgart, Pfaffenwaldring 9, D-7000 Stuttgart 80, Germany

Received 6 December 1993, in final form 28 February 1994, accepted for publication 8 March 1994

**Abstract.** The paper reports the design, development and characterization of an electro-optical equipment suitable for distance measurements and three-dimensional gauging of surfaces of industrial interest. The equipment comprises a dual-wavelength heterodyne interferometer for absolute distance measurements with a range of 20 m and an accuracy of 0.1 mm, that is integrated with a macroscopic scale, adaptive profilometer for three-dimensional measurement of the shape to 1 mm. The performance of the equipment is well suited for effective operation in industrial metrology. The equipment has been developed by three partners, namely the Dipartimento di Elettronica per l'Automazione of the University of Brescia, the Sezione Diagnostica Elettroottica of CISE, Milan, and the Institut für technische Optik of the University of Stuttgart, in the framework of a European Project partially funded by the Community Bureau of Reference.

## 1. Introduction

In modern industrial metrology there is a growing need for non-contact, accurate instrumentation to monitor the distance of a target in an absolute way, as well as to gauge the target profile and to provide a three-dimensional reconstruction of its shape. Quality control of a product, carried out either in- or post-process, and the possibility of tracking a robot arm during operation for error compensation, are typical areas of interest for this instrumentation.

Absolute interferometry, that makes use of multiple-wavelength operation and heterodyne detection, is a rapidly emerging technique for remote measurement of target distance with an extended non-ambiguity range (NAR) [1-10]. This technique can be used on both cooperative targets (retroreflectors, 'scotch-lite' ribbon) and non-cooperative targets (diffusive surfaces). Several laser sources can be used to build up an absolute interferometer. Among them, semiconductor lasers are appealing for their performance-to-cost ratio.

Three-dimensional profilometry can be developed using projection of fringes and successive deconvolution of the deformed pattern [11]. The ability to change the pattern topography yields further enhancement to the technique. Liquid crystal projectors [12, 13] are particularly suitable for adaptive fringe projection on a macroscopic scale.

Profilometry operated on a whole-field basis effectively integrates profilometry operated on a scanning basis. Availability of an absolute measuring technique is essential to sample the surface of interest at a convenient number of points with sufficient accuracy, while performing profilometric measurements on the whole surface.

The present paper gives an outline of the results obtained from the activity carried out by our laboratories in development of the combined electro-optical equipment within the framework of the European Project 'Metrology for Automated Manufacturing Processes' funded by the European Community through the Community Bureau of Reference (BCR). The paper deals with the design, development, characterization and integration, of (i) an absolute distance meter, based on a dual wavelength interferometer with heterodyne detection (DH); (ii) a three-dimensional profilometer based on the above dual-wavelength interferometer, able to provide absolute measurements at convenient points of the target; and (iii) a three-dimensional macroprofilometer based on the projection of light patterns by means of a liquid crystal projector.

The specifications of the items developed are: (i) a measuring range of up to 20 m; (ii) a depth resolution of 0.1 mm; and (iii) a data acquisition rate of up to ten measurements per second.

A detailed description of the activities carried out in

the course of the project is made in the final report, which has been submitted to the Community, and which shall be published in due time by the Community itself [14]. The researchers involved in the project are listed in the appendix.

**2. Development of an absolute laser distance meter**

**2.1. Optical layout of the DHM set-up**

The principle of operation of a dual-wavelength heterodyne interferometer has been discussed in the recent literature [9,10]. Two beams of different wavelength feed the interferometer. Each beam is, in turn, heterodyned by means of an acousto-optical modulator. All four beams feed (i) a measure interferometer, and (ii) a reference interferometer. The former contains, as one of its arms, the distance to be measured. The latter is used to compensate for all phase errors arising from the common optical paths.

In the dual-wavelength heterodyne interferometer, the distance  $\Delta L$  is measured using, as a unit of measure, the synthetic wavelength  $\lambda_{\text{synt}}$ , given by the combination of the two primary laser frequencies as

$$\lambda_{\text{synt}} = \frac{(c/f_1)(c/f_2)}{(c/f_1) - (c/f_2)} \quad (1)$$

Two configurations have been developed for the generation of the two primary wavelengths feeding the distance measurement system. These are (i) the combination of a single semiconductor laser and a high-frequency acousto-optical modulator, and (ii) a set of two semiconductor lasers, locked in frequency.

The optical breadboard of the DHM interferometer is

shown in Figure 1. A semiconductor laser (single-mode, index-guided) peaked at 780 nm is used as the primary wavelength for the interferometer. The laser beam, shaped by a pair of anamorphic prisms, enters an acousto-optical modulator for generation of the secondary wavelength shifted by 500 MHz with respect to the primary wavelength. An optical isolator is used at the output of the laser diode to prevent reflections re-entering the laser.

As an alternative source of the two wavelengths, a set-up consisting of the two frequency-locked diode lasers is also shown in figure 1. It will be described in detail in the next subsection. Either wavelength-pair generator (both generators share the same light path by using a couple of beam splitters) feeds the interferometer. Each wavelength is in turn split into two parts by two beam splitters. One half of the beams at the two wavelengths is sent into a single-mode optical fibre trunk, whereas the other half is sent to two intermediate frequency acousto-optical modulators (80 and 80.1 MHz respectively) to provide shifted wavelengths, and enters another optical fibre trunk. At the exit of the fibres, the two wavelength pairs, after polarization-control by means of the  $\lambda/4$ - $\lambda/2$  combination, exhibit a  $45^\circ$  polarization. They are subsequently split by polarizing beam splitters, and each feed one arm of the measurement interferometer and one of the reference interferometer.

The beams in the measurement arm are expanded and, in the case of a non-cooperative target, focused onto the target by an aberration-free camera lens. Immediately before leaving the interferometer, the beams are circularly polarized. The light scattered by the target (or reflected if the target is cooperative) interferes with the beams in the reference arm of the measuring interferometer at the detector by means of a polarizer.

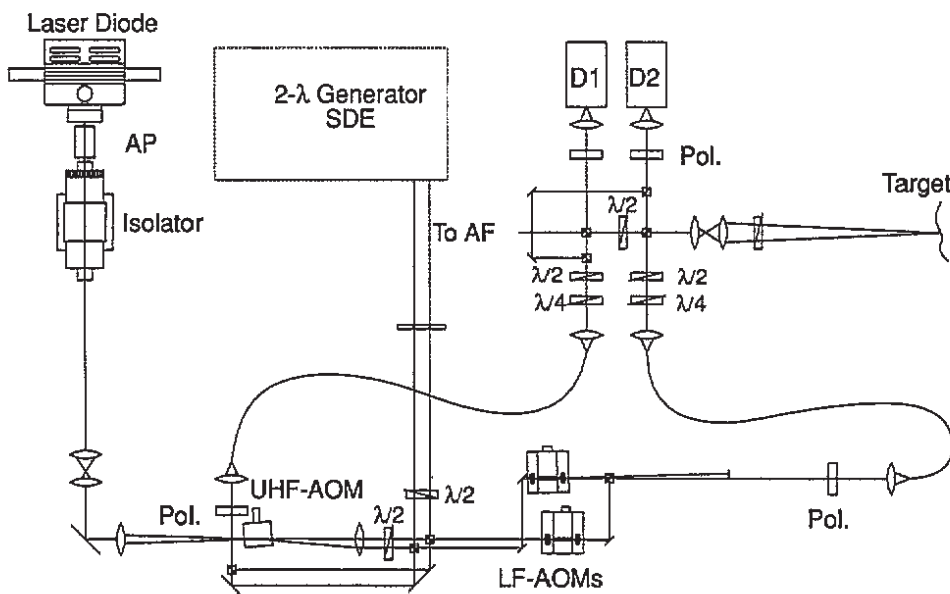


**Figure 1.** Optical layout of the dual-wavelength heterodyne interferometer breadboard set-up. UHF-AOM, ultra-high-frequency 500 MHz acousto-optical modulator; AOMs, acousto-optical modulators (80 and 80.1 MHz respectively); BS, beam splitter; PBS, polarizing beam splitter; and  $\lambda/2$  and  $\lambda/4$ , retarding plates.

The outputs from the photodiodes of both the reference and the measurement interferometer are sent to the two input channels of a digital phase meter with AGC control and demodulation stages. Recalling that the signals at the output of the demodulator are at a frequency of 100 kHz (the difference between the low-frequency acousto-optical modulators) and given the specification that the phase should be measured to one part in  $3 \times 10^4$ , a phase meter has been expressly developed by one of the partners.

## 2.2. Synthetic wavelength generation using frequency-locked diode lasers

The detailed lay-out of the generator of wavelength  $\lambda_{\text{syn}}$  using two locked diode lasers is described in figure 2. Two laser diodes operating on a single transverse mode at 780 nm have been selected. A fundamental feature, for application to the DHI, is the dependence of the laser operating wavelength on the injection current. A typical value for the diode laser optical frequency modulation as a function of the injection current is about  $3 \text{ GHz mA}^{-1}$ .

The output beams of the two semiconductor lasers are sent to two beam splitters (90%–10%). The fractions of the two beams are then recombined at the 50%–50% beam splitter, and sent to the detector. Optical isolators are used to obtain a degree of optical isolation (40 dB) high enough to avoid source instabilities due to optical feedback.

For preliminary testing and characterization of the generator of wavelength  $\lambda_{\text{syn}}$ , one of the two outputs of the beam splitter cube is sent to a polychromator and then to an optical multichannel analyser (OMA), while the other one is sent to an avalanche photodiode (APD) and then to a spectrum analyser. The OMA resolution is 30 GHz; the APD is a Telefunken BPW 28 with a bandwidth of 0–2 GHz. By adjusting the temperature and

current of one of the two sources it is possible to obtain a beat signal that is detected by the APD. A full-width at half-maximum (FWHM) of the beat signal spectrum of about 30 MHz has been achieved.

The centre frequency of the beat signal spectrum is characterized by a drift of some hundreds of megahertz over a time of 1 s: this phenomenon is due to residual temperature fluctuations of the sources. Operation of the locked sources has been achieved and its performance has been demonstrated by using an Allan variance meter [15].

## 2.3. Displacement measurements and traceability

Figure 3 shows a typical long-term stability measurement obtained with the DHI system using a cooperative target (corner cube retroreflector) placed at 5 m. For these measurements, a single-laser and acousto-optical modulator generation scheme has been used. The integration time has been set to 100 ms for each measurement. The duration of the measurements is 5 min and the corresponding RMS phase deviation is 0.11 mm. Figure 4 shows a stability measurement on a reflex foil (3M Scotch lite) at a distance of 25 m. The RMS phase value is 0.20 mm, the integration time for one phase value is 100 ms and the overall measurement duration is 30 s.

A commercial interferometer (HP 5526A single-wavelength heterodyne interferometer) with a resolution well below  $1 \mu\text{m}$  has been used to measure the accuracy of the DHI set-up. Traceability is ensured since the interferometer complies with international calibration standards. All displacement measurements have been performed on an optical bench of length 1 m. The object to be measured (corner cube or rough surface) and a second corner cube for the HP interferometer, were

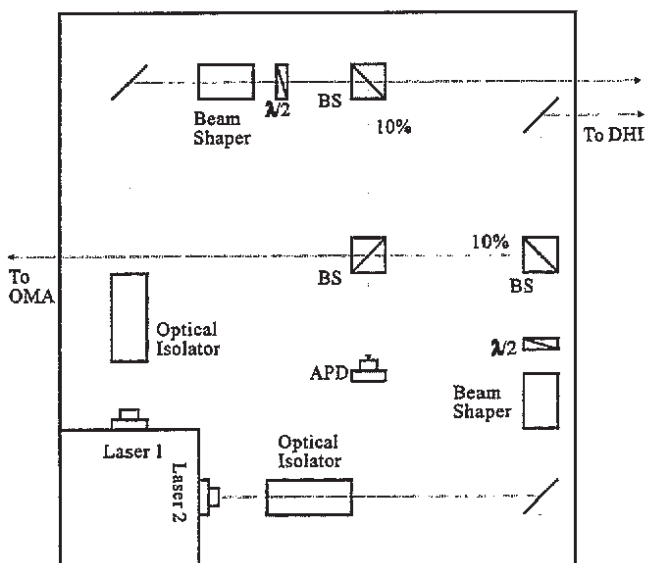


Figure 2. Lay-out of the dual-wavelength generator based on two frequency-locked laser diodes.

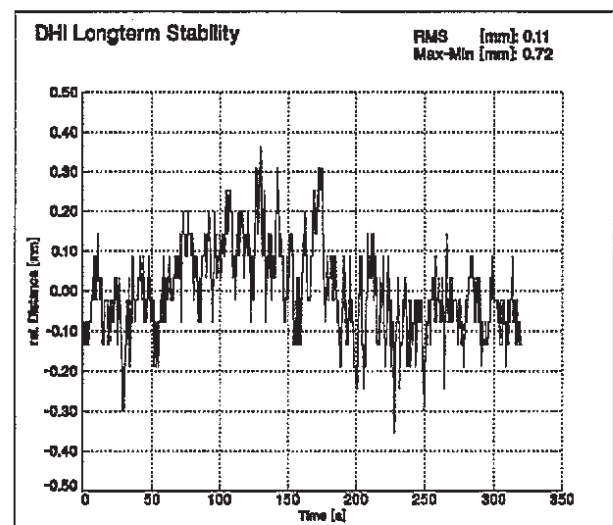


Figure 3. Long-term stability measurements of the dual-wavelength heterodyne interferometer using a cooperative target (corner cube retroreflector). Measuring time 5 min, integration time 100 ms. The root mean square distance fluctuation is 0.11 mm.

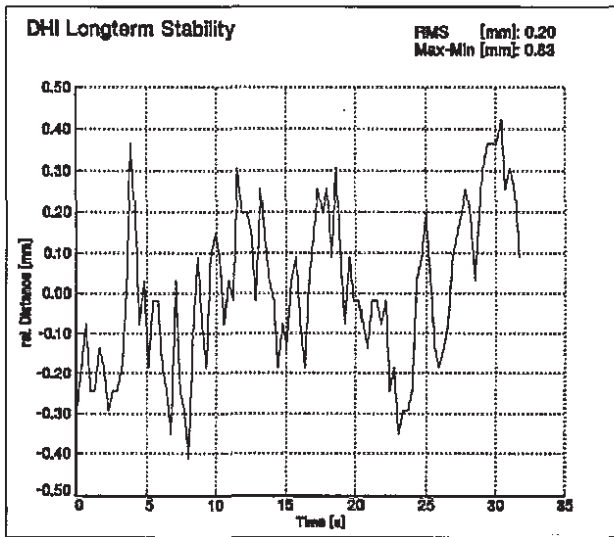


Figure 4. A 30 s stability measurement of the dual-wavelength heterodyne interferometer using a rough surface at 25 m. The integration time is 100 ms. The root mean square distance fluctuation is 0.20 mm.

placed on an optical bench mount. Figure 5 shows a sketch of the displacement measurement arrangement. The rays of both interferometers are adjusted to each other by means of iris diaphragms over a distance of 25 m. The optical bench tilt has been measured with an auto-collimating telescope and yielded an angular gap of 4 arcmin. An estimation of the maximum possible error between DHI and HP measurements yielded 0.02 mm if the visual pin-hole adjustments had an accuracy of  $\pm 1$  mm.

Figure 6 shows a measurement of a repeated shift of 750 mm of a corner cube. The upper curve shows the course of the measurement, whereas the lower diagram shows the corresponding deviations of the mean values obtained by the DHI against HP values. The repeatability is of the order of 0.1 mm. Each step consists of 30 measurements. Besides the repeatability, the lower diagram shows a systematic error of 1 mm, which also occurred with other shift measurements at several dis-

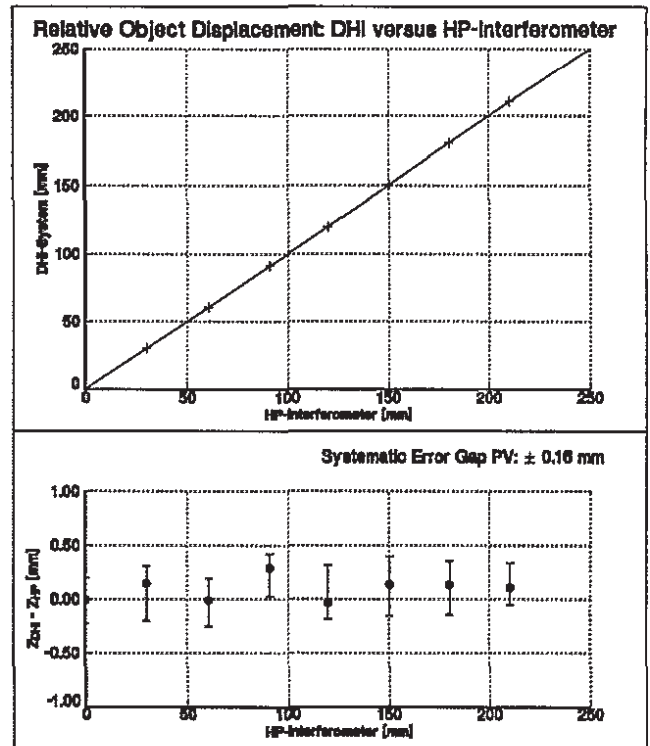


Figure 6. Mean and standard deviations of the errors for experimental points obtained by operating the dual-wavelength heterodyne interferometer using the HP interferometer as a reference.

tances. This systematic error showed no obvious linear or periodic dependence on the distance. Shift measurements with fixed focusing position of the transmitting/receiving optics showed a considerably reduced systematic error.

In order to show the ability of the interferometer to measure on moving rough surfaces, the corner cube shown in figure 4 was replaced by a rotating shaft. Figure 7 shows the corresponding displacement measurement over a range of 30 cm without changing the focusing position of the optics.

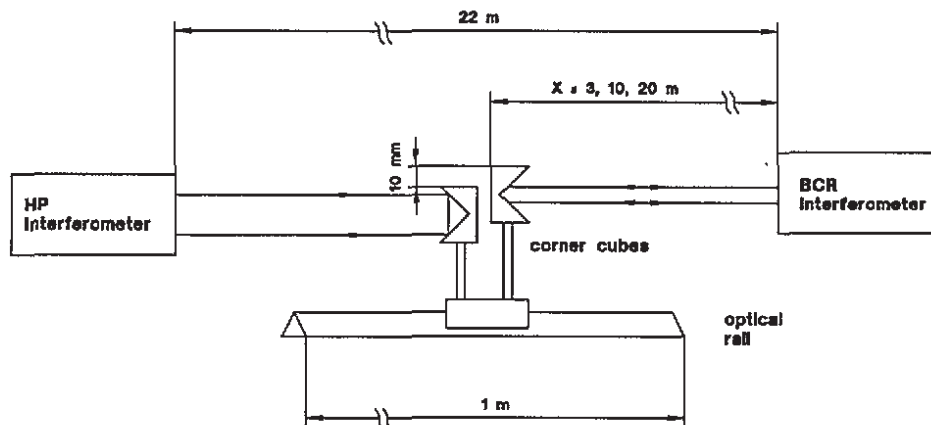


Figure 5. Experimental arrangement of the displacement measurements performed to ensure traceability of absolute measurements.

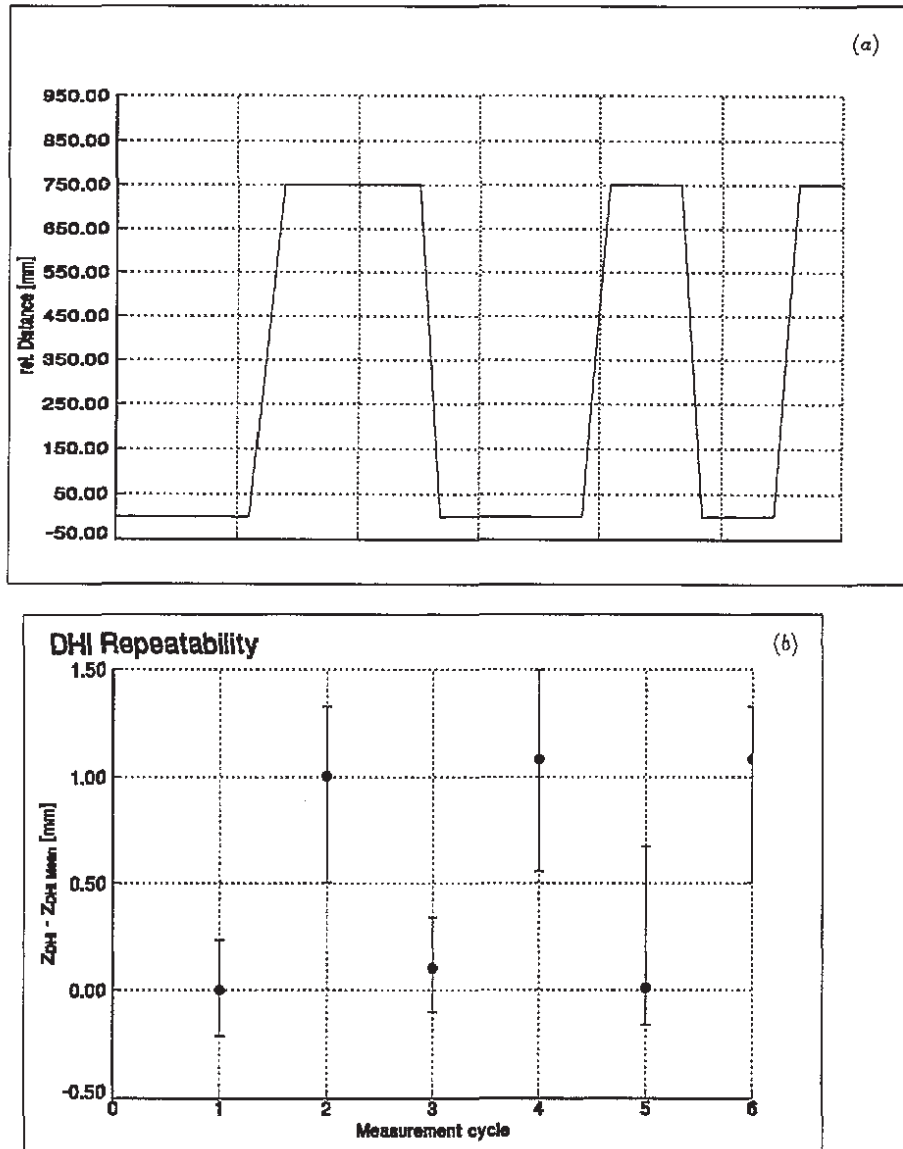


Figure 7. (a) plot of repeated displacement measurement of a distance of 750 mm. (b) the error bars and circles signify the range and mean values of the dual-wavelength heterodyne interferometer measurements obtained for each position.

### 3. Development of a macroscopic profilometer

#### 3.1. Development of a scanning and autofocus unit for the DHI set-up

The DHI system described in the previous section has been combined with (i) a scanner unit and (ii) an autofocus unit, to provide a non-contact point-by-point profilometer. The scanning system used is a commercial unit with an angular range of  $40^\circ$ , and a repeatability of 0.05%. The developed autofocus unit is shown in figure 8. A small fraction (approximately 10%) of the light back-scattered by the target is taken out from the main path through beam splitter BS and is sent to an optical system composed of a spherical and a cylindrical lens. The optics focus the laser spot at the target onto a four-quadrant detector. The distance between the astigmatic optics and the detector is adjusted so that the image on the detector is a circular spot when the DHI

measurement beam is focused onto the target. This distance defines the so-called best focus plane. When the measurement beam focuses before or behind the target, the image on the detector is an elliptical spot, whose principal axes are oriented along the horizontal or vertical direction respectively. The output signals from the quadrant detector are digitized by a personal computer by means of a plug-in A/D acquisition board. A computation is performed in order to evaluate the amplitude and the sign of the error signal and to drive the stepping motor, which in turn drives the objective.

#### 3.2. Development of a macroprofilometer based on structured light projection

Macroprofilometry using projected fringes is an established optical technique, although not fully exploited in industrial metrology due to some as yet unresolved

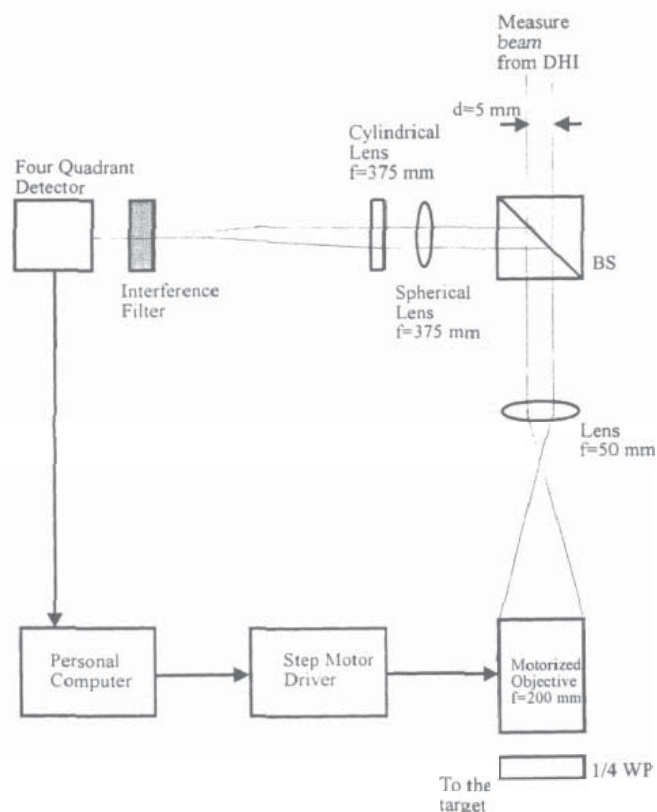


**Figure 8.** Experimental set-up for the autofocus device. WP, wave-plate and BS, beam splitter.

technical problems. In structured light projection, the projection of a grating onto the surface to be measured, and the observation of the resulting pattern from a different perspective, produce a deformed pattern, according to the topography of the object. In order to extract the three-dimensional topographic information, the two-dimensional deformed image has to be acquired by a video camera and properly elaborated [16].

The complexity of the target to be analysed, and the presence of shadow regions along preferred directions, suggest the use of adaptive patterns. This holds true particularly whenever phase-shifting or frequency modulation of the grating are accomplished. Problems related to the shift of the grating to be projected (precision of motion and speed of elaboration) may be solved by the adaptivity of the projected patterns. Furthermore, adaptivity decreases the limit in resolution due to the slope of the object, connected to the pitch (period) of the grating.

A schematic diagram of the profilometer is shown in figure 9. Both the video camera and the projector are at distance  $L$  from plane  $R$ , on which the object to be measured is placed. This plane represents a reference for the profile measurement of the object. The projection and imaging units are at distance  $d$  from each other, and  $W$  is the width of the illuminated area. Use of a LCD projector allows one to project flicker-free, long-term stable and well-contrasted gratings of variable period. The projector is directly controlled by a personal

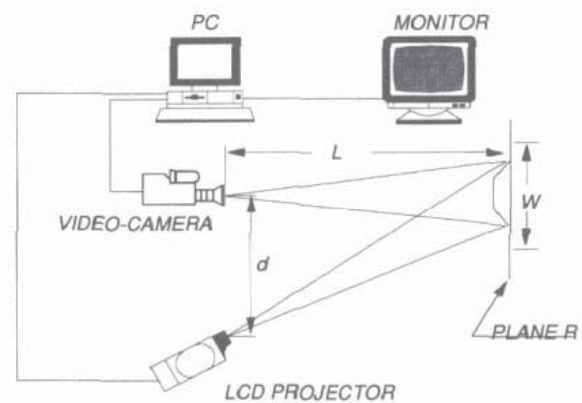


**Figure 9.** Whole-field macroprofilometer lay-out using the liquid crystal projector unit.

computer: this enables one to adapt the grating to the shape of the object (by modifying its period on-line). The projected pattern is acquired by a black and white CCD video camera. It acquires images with a resolution of  $512 \times 512$  pixels. The images are grabbed and stored by dedicated boards plugged into the personal computer (PC).

Evaluation and testing of image pre-elaboration algorithms have been performed. In particular the effectiveness of morphological algorithms (such as erosion and dilation) in enhancing the recorded image has been evaluated. Noise reduction by means of averaged acquisition, background subtraction and gray-level normalization to the projection intensity have been developed [17]. Profile reconstruction is performed by a suitable demodulation algorithm [18].

### 3.3. Performance evaluation of the macroprofilometer

To test the profilometer, a flat surface has been used as a reference plane in the profile measurement. A special surface treatment guarantees a light gray-painted, uniformly diffusive surface, which results in good-quality images. Moreover, reduced weight simplifies the system assembly.

A three-dimensional surface to be used as a master for the calibration of the whole-field profilometer has been prepared. The master has been designed to be manageable, dimensionally stable and lightweight. To be used as a reference this surface has been gauged using a traceable contact measurement machine (CMM). It has been verified that the object deformations are below 0.1 mm. A coordinate system has been chosen for the object. This has been used to evaluate both the measurements performed by the CMM system and those resulting from the whole-field profilometer. Measurements from both the CMM and the optical profilometer have been evaluated and compared with respect to correspondence of 36 selected points on the master surface. A statistical analysis of the measurement errors has been performed. In the case of maximum grating contrast, the system

accuracy is 0.09% in depth with a precision of 0.1% in measurement range.

In order to merge DHI profilometer measurements with whole-field profilometer measurements, a suitable procedure has been implemented to measure the relative position and orientation of the coordinate frame of the two systems. The procedure is based on the following steps.

- (i) The DHI profilometer sets its Z axis perpendicular to the reference plane of the whole-field profilometer (therefore parallel to the Z axis of the whole-field profilometer); the procedure is automatic and based on triangulation.
- (ii) The DHI spot is directed towards a series of points on the reference plane: for each point the spot is recognized by the whole-field profilometer camera. A simple elaboration of the data gives the relative shifts as well as the relative orientations of the X and Y axes of the two coordinate systems.
- (iii) The absolute distance of the reference plane is measured by the DHI system and stored as the zero quote: the subsequent Z quotes are then measured with respect to this zero.

Following identification of the relative position and orientation, the two systems are ready to measure surface profiles in a cooperative way. A connection procedure has been performed, whereby the whole-field profilometer acts as the master and the DHI profilometer as the slave. Thus, data coming from the DHI profilometer can be easily integrated with those from the whole-field profilometer.

As a first step, the DHI profilometer, obtained from the combination of the single-point DHI, scanner and autofocus system, has been tested. Figure 10 shows the result of a session of test and characterization of the integrated combined equipment. Figure 10(a) shows the two-dimensional lay-out of a target which consists of a portion (250 mm × 250 mm) of the plane used as the reference, with a sequence of traceable Johnson blocks of different heights superimposed on it. The target was measured using the DHI profilometer alone. Figures 10(b) and (c) show, respectively, the three-dimensional plot of the measured height values and of their standard deviations. It is evident from comparison of figures 10(b) and (c) that the accuracy of the measurement remains within the specified limits.

Finally, the combined distance and surface profile

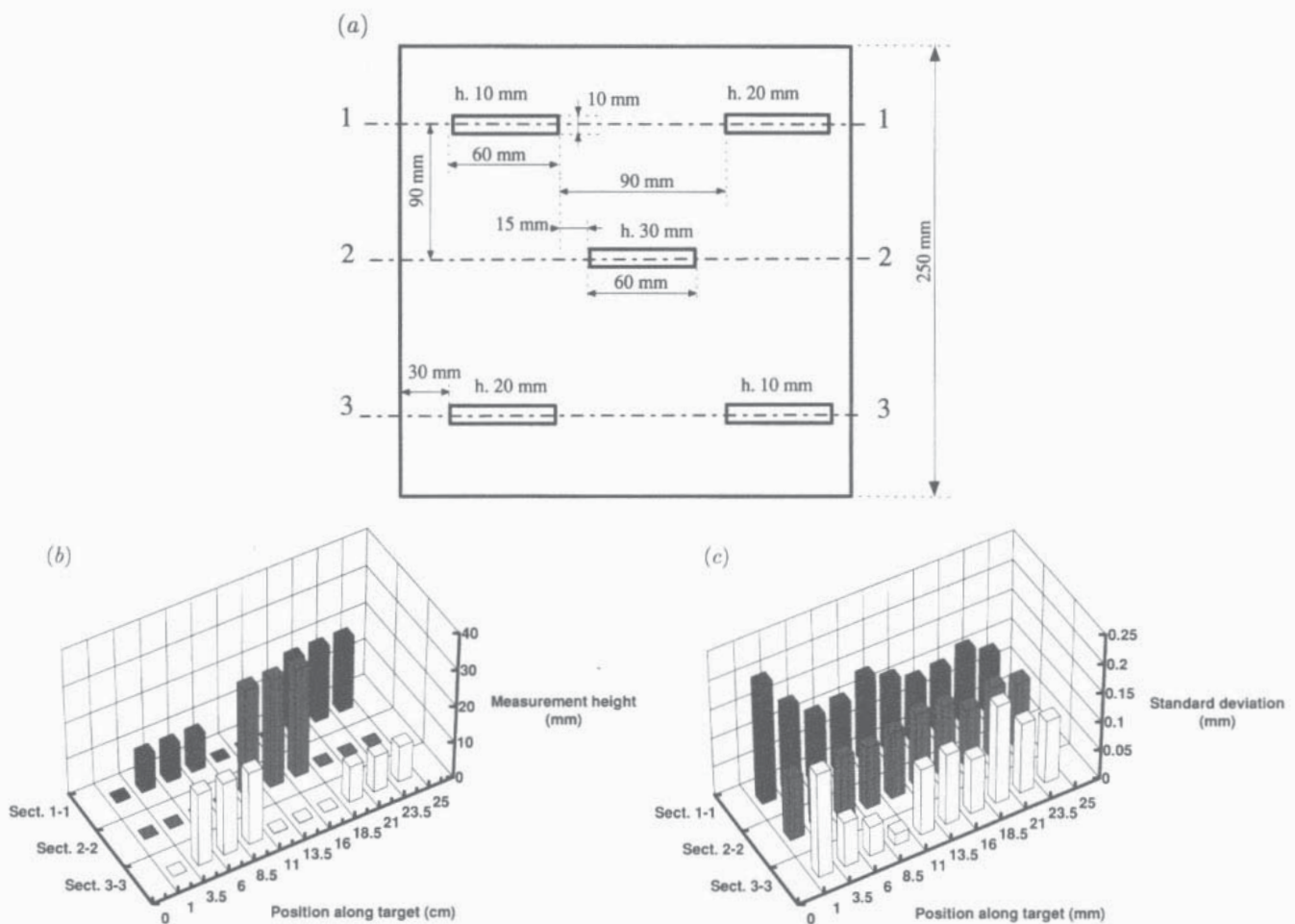


**Figure 10.** (a) Lay-out of the target designed for characterization of the equipment. (b) Measurements of the absolute heights in correspondence to the sections drawn in (a), (c) Measurements of the standard deviations of the measured heights in correspondence with the sections drawn in (a).

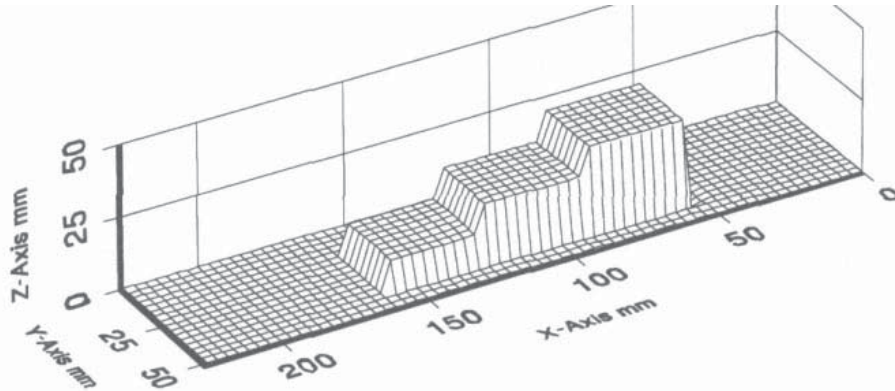


**Figure 11.** Three-dimensional profile of a target obtained with the projected fringe macroprofilometer. Standard deviations of the height measurements from the dual-wavelength heterodyne interferometry profilometer are 0.12 mm at  $(x=60, y=25)$ , 0.099 mm at  $(x=100, y=25)$  and 0.11 mm at  $(x=150, y=25)$ .

measurement system has been characterized and tested. Figure 11 shows a three-dimensional plot of the profile of a combination of Johnson blocks similar to that of figure 10(a) in correspondence with selected points within the surface scanned using the projected fringe macroprofilometer. Standard deviations of the height measurements from the DHI profilometer are 0.12 mm (the height is 30 mm at  $x=60, y=25$ ), 0.099 mm (the height is 20 mm at  $x=100, y=25$ ) and 0.11 mm (the height is 10 mm at  $x=150, y=25$ ).

#### 4. Conclusions

A combined electro-optical system has been described for long-range, high-accuracy, absolute measurement of distance and profiles. From the measurements performed on individual subsystems, and from those performed on the integrated equipment, it has been shown that the combined distance and surface profile equipment fulfills the specifications agreed with the Community at the beginning of the project, and is potentially very useful for the industrial applications envisaged, although further developments need to be performed to achieve a lay-out suitable for industrial purposes.

#### Acknowledgments

The present work has been partially supported by the European Community, Bureau of Community Reference, under contracts 3332/1/0/162/89/9-BCR-I(30) I(31) and D(32).

A list of all the research and development staff involved in the project follows. The project coordinator acknowledges the skillful and competent contribution of all of them.

- (i) Dipartimento di Elettronica per l'Automazione, Università degli Studi di Brescia: Franco Docchio,

Umberto Minoni, Giovanna Sansoni, Enea Gelmini and Luca Biancardi.

- (ii) Sezione Diagnostica Elettroottica, CISE SpA, Milano: Umberto Perini, Giuseppe Re Garbagnati, Enrico Paganini, Lorenzo Spadoni and Vieri Piemontese.
- (iii) Institut für technische Optik, Universität Stuttgart: Hans Tiziani, Zoran Södnik, Edgar Fischer, Ernst Dalhoff, Thomas Ittner and Silke Kreuz.

#### References

- [1] Williams C C 1986 Optical ranging by wavelength multiplexed interferometry *J. Appl. Phys.* **60** 1900-3
- [2] Massie N A 1987 Absolute distance interferometry *SPIE Interferometric Metrology* **816** 149-57
- [3] Walsh C J 1987 Measurements of absolute distances to 25 m by multiwavelength CO<sub>2</sub> laser interferometry *Appl. Opt.* **26** 1680-7
- [4] Chen J, Ishii Y and Murata K 1988 Heterodyne interferometry with a frequency-modulated laser diode *Appl. Opt.* **27** 124-8
- [5] Bien F, Camac M, Caulfield H J and Ezekiel S 1981 Absolute distance measurements by variable wavelength interferometry *Appl. Opt.* **20** 400-3
- [6] Matsumoto H 1986 Synthetic interferometric distance measuring system using a CO<sub>2</sub> laser *Appl. Opt.* **25** 493-8
- [7] Cheng Y Y and Wyant J C 1984 Two-wavelength shifting interferometry *Appl. Opt.* **23** 4539-43
- [8] Cheng Y Y and Wyant J C 1985 Multiple-wavelength phase-shifting interferometry *Appl. Opt.* **24** 804-7
- [9] Dändliker R, Thalmann R and Prongué D 1988 Two-wavelength laser interferometry using superheterodyne detection *Opt. Lett.* **13** 339-41
- [10] Södnik Z, Fischer E, Ittner T and Tiziani H J 1991 Two-wavelength double heterodyne interferometry using a matched grating technique *Appl. Opt.* **30** 3139-44
- [11] Tang S and Hung Y Y 1990 Fast profilometer for the automatic measurement of 3-D object shapes *Appl. Opt.* **29** 3012-8
- [12] Liu H K and Chao T H 1989 Liquid crystal television spatial light modulators *Appl. Opt.* **28** 4772-80



- [13] Sansoni G, Docchio F, Minoni U and Bussolati C 1991 Development and characterization of a liquid crystal projection unit for adaptive structured illumination *Proc. SPIE* **1614** 78–86
- [14] Docchio F, Biancardi L, Minoni U, Sansoni G, Perini U, Musazzi S, Piemontese V, Spadoni L, Tiziani H, Fischer E, Dalhoff E and Kreutz S 1993 Multisensor electro-optical equipment for automated manufacturing systems Final Report of the European Project, to be published
- [15] Allan D W 1966 Statistics atomic frequency standards *IEEE Proc.* **54** 221–30
- [16] Sansoni G, Docchio F, Minoni U and Biancardi L 1992 Adaptive profilometry for industrial applications *Proc. 17th NATO Course on Laser Applications to Mechanical Industry, Erice* pp 351–64
- [17] Sansoni G 1993 A novel, adaptive system for 3-D optical profilometry using a liquid crystal projector *IEEE Trans. Instrum. Meas.* to be published
- [18] Sansoni G, Biancardi L, Docchio F and Minoni U 1993 Comparative analysis of low-pass filters for the demodulation of projected gratings in 3-D adaptive profilometry *IEEE Trans. Instrum. Meas.* submitted